

Adaptive Bearing-Only Formation Tracking Control for Nonholonomic Multiagent Systems

Xiaolei Li¹, Changyun Wen¹, *Fellow, IEEE*, Xu Fang¹, and Jiange Wang¹

Abstract—In this article, we consider the formation tracking problem of nonholonomic multiagent systems only using relative bearing measurements between the agents. Such a practical and important yet challenging issue has been taken into limited consideration by existing approaches, which usually requires additional measurements such as relative positions. The contributions of this article are two-fold. First, a fully distributed reference velocity estimator is proposed. Under the proposed adaptive estimator, each agent can estimate the time-varying reference velocity asymptotically. Second, an input-to-state stable controller is designed according to the bearing rigid theory. Under the proposed controller, the formation with bearing-only constraints can be achieved. Finally, the proposed scheme is demonstrated and its effectiveness is verified by presenting some simulation and experimental tests.

Index Terms—Adaptive observer, bearing-only measurement, formation tracking, multiagent systems.

I. INTRODUCTION

ADDRESSING issues related to consensus aims to seek an agreement among all the involved multiple agents, which has been widely used to solve the problems of formation control [1], [2]; distributed estimation of the wireless-sensor network [3]; and distributed optimization [4]. As one of the typical applications of consensus, formation control of multiagent systems is to make the agents converge to a given geometric shape. It has been successfully applied to satellite formation [5], [6]; robot formation [7]–[11]; area coverage of the wireless-sensor network [12], [13]; etc. According to different goals, formation control can be divided into static formation [14] and formation tracking [15]. How to achieve stable formation for different purposes is still one of the hot issues in the control field [16].

As mentioned in [16], according to different measurements from the sensors, the formation control approach is generally

divided into three categories: 1) position-based; 2) distance-based; and 3) bearing-based approaches. A position-based control always needs real-time position measurements in a global framework from a global positioning system (GPS)-like system, while a distance-based approach usually requires relative position measurements. Compared to the other two approaches, the bearing-based approach has a natural connection with the vision measurements that are widely used in robotic systems, since visual servo control plays an important role in robot navigation and positioning tasks, which makes the bearing-based formation control of the multiagent system be an attractive area [17]. When the relative position information is not needed, the bearing-based control approach degenerates into the bearing-only method. A bearing-only method puts the minimum requirements on the system hardware, such as camera onboard [17] or sensor arrays [18], [19] and, thus, it has received much attention recently. For instance, a class of formation control laws is proposed for some specified shapes [20]–[23]. Zhao and Zelazo [24] proposed a bearing-only formation control law for linear first-order multiagent systems according to the proposed bearing rigidity theory. Then, they extended the control law to solve the directed formation control problem defined in SE(2) space [25]. By combining with the relative position measurements, the bearing-based approach has also received some attention [26], [27]. However, most existing bearing-only and bearing-based approaches can only be used to solve the formation control problem of linear multiagent systems modeled by single-integrator or double-integrator kinematics. It is significant to investigate the bearing-only formation control problem of nonholonomic multiagent systems.

In addition to the system kinematic constraints, formation tracking control is another practical issue in some applications, such as autonomous navigation and target tracking. For example, a time-varying formation tracking problem is addressed for a class of linear multiagent systems with multiple leaders by using the relative displacement measurements in [28]. In [29], a leader–follower formation tracking control law is proposed based on the linear quadratic regulation and robust compensation theory for a class of double-integrator systems. Then, the formation tracking problem is considered for single-integrator multiagent systems using distance and local displacement measurements [30]. However, the mentioned approaches always need the relative position measurements. How to use the bearing-only measurements to achieve formation tracking control is still unsolved due to its difficulty of handling nonlinearities. Very recently, a novel

Manuscript received June 1, 2020; revised October 2, 2020; accepted December 1, 2020. This work was supported in part by the Ministry of Education (MOE), Singapore under Grant MOE2017-T2-1-050 and Grant MOE2020-T1-1-067, and in part by the National Natural Science Foundation of China under Grant 61903319. This article was recommended by Associate Editor J. Chen. (Corresponding author: Jiange Wang.)

Xiaolei Li, Changyun Wen, and Xu Fang are with the School of Electrical and Electronic Engineering, Nanyang Technological University, Singapore (e-mail: xiaolei@ntu.edu.sg; ecywen@ntu.edu.sg; fa0001xu@e.ntu.edu.sg).

Jiange Wang is with the School of Electrical Engineering, Yanshan University, Qinhuangdao 066004, China (e-mail: jg_wang@163.com).

Color versions of one or more figures in this article are available at <https://doi.org/10.1109/TCYB.2020.3042491>.

Digital Object Identifier 10.1109/TCYB.2020.3042491

bearing-only formation tracking control law is proposed by assigning the desired velocity to the agents [15]. Besides the leader–follower approach, an observer-based approach can also be used to the bearing-only formation tracking, which is still unsolved.

In this article, we consider the formation tracking problem of nonholonomic multiagent systems by only using the relative bearing measurements between the agents. In order to achieve the formation tracking with the desired bearing constraints, the concept of bearing rigid graph is used to describe the target formation. An adaptive fully distributed observer is proposed to estimate the time-varying desired velocity. Then, an input-to-state stable control law is designed according to the velocity estimate and bearing-only measurements. To demonstrate the effectiveness of the proposed control law, both simulation and experimental tests using robots are presented, which hence provides a practical solution to the formation tracking problem in robotic systems. The contributions of this article are given as follows.

- 1) An adaptive fully distributed observer is proposed to estimate the desired velocity. Compared with [31] and [32], which need the assumption that the bound of the desired velocity is known for design and implementation, the proposed adaptive observer with a dynamic gain removes this assumption and can estimate the velocity asymptotically.
- 2) A novel input-to-state stable control law is proposed for nonholonomic multiagent systems based on the velocity estimates and the bearing-only measurements. Compared with [27] and [29], which require both bearing and relative position measurements, only the bearing measurements are used in the proposed control law.

The outline of this article is given as follows. Section II proposes the preliminaries on the bearing rigid theory and formulates the formation tracking problem. In Section III, the fully distributed observer and formation tracking control law are proposed. Some simulation results and experiments are presented to verify the proposed control scheme in Section IV. Section V concludes this article and some future directions are also presented therein.

II. PRELIMINARIES AND PROBLEM FORMULATION

A. Preliminaries: Bearing Rigidity

The first issue for the formation control problem is to determine when the target formation is unique. In this article, the bearing rigid theory will be used to uniquely determine the target formation and the related concepts are given in this part. Some basic notations and symbols are given in Table I.

Note that the topology $\mathcal{G} = (\mathcal{V}, \mathcal{E})$ is undirected. The rows and columns of its incidence matrix \mathcal{H} are indexed by edges and vertices, respectively. $[\mathcal{H}]_{ki} = 1$ corresponds to the edge $k \in \mathcal{E}$ with node i being the head, $[\mathcal{H}]_{ki} = -1$ if node i is the tail of edge $k \in \mathcal{E}$, and $[\mathcal{H}]_{ki} = 0$ otherwise. Assume that positions of the multiagent systems do not coincide with each other, that is, $p_i \neq p_j$. For the relative bearing g_{ij} between agents i and j , we have $g_{ij} = -g_{ji}$ and $\|g_{ij}\| = 1$. Before exploring the bearing rigidity theory, the following bearing

TABLE I
NOTATIONS AND SYMBOLS

Symbols	
\mathbb{R}, \mathbb{R}_+	Real and positive real number set
$\mathbb{R}^n, \mathbb{R}^{n \times n}$	n-dimensional vector and matrix space
$I_n \in \mathbb{R}^{n \times n}$	n-dimensional identity matrix
$\ \cdot\ $	Euclidian norm of a vector or a matrix
$\lambda(A)$	Eigenvalue of matrix A
$\text{Rank}(A)$	Rank of matrix A
\otimes	Krocker product
$\cap_{\mu(\bar{E})=0}$	Intersection over all sets \bar{E}
Notations	
$\mathcal{V} = 1, 2, \dots, N$	Index set of the agents
$\mathcal{E} \in \mathcal{V} \times \mathcal{V}$	Edge set between the agents
$\mathcal{G} = (\mathcal{V}, \mathcal{E})$	Communication/sensing topology
\mathcal{N}_i	Neighbor set of agent i
$(i, j) \in \mathcal{V}$	Information flow between agent i and j
$\mathcal{H} = [\mathcal{H}]_{ij} \in \mathbb{R}^{m \times n}$	Incidence matrix of $\mathcal{G} = (\mathcal{V}, \mathcal{E})$
$\mathcal{L} = [a_{ij}]$	Laplacian matrix of $\mathcal{G} = (\mathcal{V}, \mathcal{E})$
\mathcal{D}	Pinning matrix of $\mathcal{G} = (\mathcal{V}, \mathcal{E})$
$p_i \in \mathbb{R}^2$	Position of the i -th agent
$e_{ij} = p_j - p_i$	Relative position between agent i and j
$g_{ij} = e_{ij} / \ e_{ij}\ $	Relative bearing between agent i and j
g_{ij}^*	Desired bearing constraints
$\mathcal{B}(p) \in \mathbb{R}^{dm}$	Bearing function of (\mathcal{G}, p)
$\mathcal{R}(p) : \mathbb{R}^{dN} \rightarrow \mathbb{R}^{dm}$	Bearing rigidity matrix of (\mathcal{G}, p)
$B(x, \delta)$	Open ball with radius δ centered at x
$\text{co}(X), \bar{\text{co}}(X)$	Convex and convex closure of set X

orthogonal projection operator $P : \mathbb{R}^d \rightarrow \mathbb{R}^{d \times d}$ is first given as:

$$P_{g_{ij}} \triangleq I - g_{ij}^T g_{ij} \quad (1)$$

which has the property that $P_{g_{ij}}^2 = P_{g_{ij}}$ and $P_{g_{ij}} g_{ij} = 0$. Its geometric meaning is to map the vector to the direction perpendicular to it.

In order to uniquely determine a geometric configuration using the bearing constraints $\{g_{ij}^*\}_{(i,j) \in \mathcal{E}}$, rewriting the bearings as a vector in the order of the edges of the framework (\mathcal{G}, p) , the bearing function is defined as $\mathcal{B}(p) \triangleq [g_1^T, g_2^T, \dots, g_m^T]^T \in \mathbb{R}^{dm}$ where g_k corresponds to the k th edge of graph \mathcal{G} for $k \in \{1, 2, \dots, m\}$ and $p = [p_1, \dots, p_N] \in \mathbb{R}^{dN}$ is a realization of the configuration (\mathcal{G}, p) . Then, the bearing rigidity matrix $\mathcal{R}(p)$ is given as follows:

$$\mathcal{R}(p) \triangleq \frac{\partial \mathcal{B}(p)}{\partial p} \in \mathbb{R}^{dm \times dn}. \quad (2)$$

As stated in [24], the rank of $\mathcal{R}(p)$ plays an important role in uniqueness of the configuration (\mathcal{G}, p) . Specifically, $\text{rank}[\mathcal{R}(p)] \leq dn - d - 1$ if and only if the configuration (\mathcal{G}, p) is infinitesimally bearing rigid. That is, the configuration (\mathcal{G}, p) is uniquely determined by the bearing constraints. Then, consider the following isometry bijective map $\mathcal{T} : \mathbb{R}^d \rightarrow \mathbb{R}^d$

$$g_k(q) = \mathcal{T}(g_k(p)), k = 1, \dots, m$$

where map \mathcal{T} shows that the bearing measurements of configuration (\mathcal{G}, p) is essentially invariant to translation and scaling.

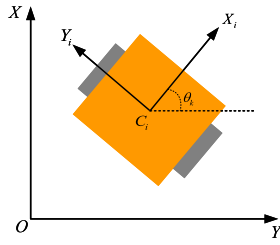


Fig. 1. Illustration of a nonholonomic agent.

In other words, (\mathcal{G}, p) and (\mathcal{G}, q) are said to be bearing equivalent if $P_{p_i-p_j}(q_i - q_j) = 0$ for $(i, j) \in \mathcal{E}$ and are congruent if $P_{p_i-p_j}(q_i - q_j) = 0$ for all $i, j \in \mathcal{V}$ [24]. This feature of the bearing rigidity allows us to focus more on formation control than how to exclude flip ambiguities. Then, the following lemma is given.

Lemma 1 (Uniqueness of (\mathcal{G}, p)) [24]: The configuration (\mathcal{G}, p) is uniquely determined up to translation and scaling if (\mathcal{G}, p) is infinitesimally bearing rigid.

This lemma essentially determines the uniqueness of the solution to the formation control [10], [24] and network localization [33], [34]. Note that $\text{rank}[R(p)] \leq dn - d - 1$ is necessary and sufficient for the uniqueness of configuration (\mathcal{G}, p) . That is, according to Lemma 1, the infinitesimally bearing rigidity of a configuration (\mathcal{G}, p) can be directly derived from the rank condition. This is significantly better than distance rigidity [35], as the flip ambiguities are naturally excluded and the almost global stability can be guaranteed by using the bearing rigidity theory.

B. Problem Formulation

Nonholonomic multiagent systems are considered, which is shown in Fig. 1. The kinematic model of the i th agent is given as follows:

$$\begin{cases} \dot{x}_{ci} = v_i \cos \theta_i \\ \dot{y}_{ci} = v_i \sin \theta_i \\ \dot{\theta}_i = \omega_i \end{cases} \quad (3)$$

where $p_i = [x_{ci}, y_{ci}]$ is the position of agent i in a global framework $\{X, O, Y\}$. θ_i denotes the heading angle in a local framework $\{X_i, C_i, Y_i\}$ relative to the global framework $\{X, O, Y\}$. The trigonometric functions are used to determine the respective components of the velocity along the X and Y axes. v_i and ω_i are linear and angular velocity, respectively.

By giving a configuration $\mathcal{G}^*(p^*) = (\mathcal{V}^*, \mathcal{E}^*)$ with the desired position p^* , the bearing constraints can be denoted by $F^*(t) = (\mathcal{G}^*, p(t))$ with $p = (p_1, p_2, \dots, p_N)$. The following assumptions is necessary for stable formation tracking.

Assumption 1: The configuration $F^*(t) = (\mathcal{G}^*, p(t))$ is infinitesimally bearing rigid.

Assumption 2: The desired velocity $v_0(t)$ and acceleration $\dot{v}_0(t)$ are both bounded.

Remark 1: Assumptions 1 and 2 are sufficient conditions to achieve bearing-only formation tracking control. Assumption 1 gives the condition that the formation configuration $F^*(t) = (\mathcal{G}^*, p(t))$ is uniquely determined by the bearing-only measurements. As stated in [35], if the configuration $F^*(t) = (\mathcal{G}^*, p(t))$

is infinitesimally bearing rigid, then the formation configuration $F^*(t) = (\mathcal{G}^*, p(t))$ is unique and the flip ambiguities are naturally excluded. Assumption 2 has been widely used, see [36] and [32], for achieving the reference velocity estimate. Note that the failure of some agents may make these assumptions untenable and result in the failure of the proposed method. However, there are some potential ways to solve this problem [37]–[40], which is out of the scope of this article and will be considered in the future.

Then, the bearing-only tracking problem is formulated as follows.

Problem 1 (Bearing-Only Formation Tracking): Design the control input (v_i, w_i) such that the nonholonomic multiagent systems (3) can track a target with desired velocity $v_0(t)$ and maintain the desired formation shape $F^*(t) = (\mathcal{G}^*, p(t))$, that is, $g_{ij} \rightarrow g_{ij}^*$ for all $(i, j) \in \mathcal{E}$ and $v_i(t) \rightarrow v_0(t)$ as $t \rightarrow \infty$.

Since only a part of the agents has access to the desired velocity, an observer will be designed for the agents to cooperatively estimate the desired velocity. To this end, the following preliminaries on nonsmooth analysis and ISS lemma are presented for the control design and convergence analysis.

For a nonlinear system $\dot{x} = f(x, t)$, the locally bounded function $f(\cdot) : \mathbb{R}^m \times \mathbb{R} \rightarrow \mathbb{R}^m$ is discontinuous and Lebesgue measurable. $x(t) \in \mathbb{R}^m$ is called a Filippov solution of $f(x, t)$ on $[t_0, t_1]$ if $x(t)$ is absolutely continuous over $[t_0, t_1]$ and satisfies the differential inclusion $\dot{x} \in \mathcal{K}[f](x, t)$ for almost all $t \in [t_0, t_1]$ with $\mathcal{K}[f] := \bigcap_{\delta > 0} \bigcap_{\mu(\bar{E})=0} \bar{co}(f(B(x, \delta) - \bar{E}), t)$. Considering a locally Lipschitz function U , its Clarke's generalized gradient is $\partial U := co\{\lim \nabla U(x_i) | x_i \rightarrow x, x_i \in \Omega_v \cup \bar{E}\}$ with Ω_v being the Lebesgue measure zero set where $\nabla U(x_i)$ does not exist and \bar{E} being a zero measure set. Then, the set-valued Lie derivative of U with respect to $\dot{x} = f(x, t)$ is given as $\dot{U} := \bigcap_{\zeta \in \partial U} \zeta^T \mathcal{K}[f](x, t)$. Now, the following lemma is valid.

Lemma 2 (Nonsmooth Barbalat's Lemma [41]): Suppose that the Filippov solution of $\dot{x} = f(x, t)$ always remains in a compact set Ω for all $t \geq t_0$. If there exists a time-independent regular function $U : \Omega \rightarrow \mathbb{R}$ with $v \leq 0 \forall v \in \dot{U}$, which is trivially satisfied if \dot{U} is an empty set, then all trajectories in Ω converge to the largest invariant set within the closure of $S = \{x \in \Omega | 0 \in \dot{U}\}$.

In addition, the following lemma will be used in the convergence analysis of the resulting overall control system.

Lemma 3 (ISS for Cascaded System [42]): Consider the following nonlinear cascaded system:

$$\begin{cases} \dot{x}_1 = f_1(x_1, x_2) \\ \dot{x}_2 = f_2(x_2) \end{cases} \quad (4)$$

where $f_1(\cdot) : \mathbb{R}^{n_1 \times n_2} \rightarrow \mathbb{R}^{n_1}$ is locally Lipschitz continuous in $x = [x_1^T, x_2^T]^T$ and $f_2(0) = 0$. If the subsystem $\dot{x}_1 = f_1(x_1, x_2)$ is ISS from the input x_2 to state x_1 and the subsystem $\dot{x}_2 = f_2(x_2)$ is globally asymptotically stable, then the cascaded system (4) globally asymptotically converges to equilibrium point $(x_1, x_2) = 0$.

III. ADAPTIVE BEARING-ONLY FORMATION TRACKING CONTROL

A. Fully Distributed Adaptive Observer Design

In this section, the following adaptive estimator of estimating reference velocity is proposed for agent i :

$$\begin{aligned}\dot{\hat{v}}_i &= - \sum_{j \in \mathcal{N}_i} c_{ij}(t) a_{ij}(t) \text{sign}(\hat{v}_i - \hat{v}_j) \\ &\quad - c_i(t) b_i(t) \text{sign}(\hat{v}_i - \hat{v}_0),\end{aligned}\quad (5)$$

$$\dot{c}_{ij} = \nu \|\hat{v}_i - \hat{v}_j\|_1, \dot{c}_i = \nu \|\hat{v}_i - \hat{v}_0\|_1 \quad (6)$$

where $\mathcal{N}_i := \{j \in \mathcal{V} : (i, j) \in \mathcal{E}\}$, $\hat{v}_i(t)$ is the estimate of $v_0(t)$ by agent i , $\hat{v}_0(t) \equiv v_0(t)$, $b_i(t)$ is the pinning gain for $i = 1, \dots, N$ with the following definition. If agent i can access the reference velocity, then $b_i(t) = 1$, otherwise $b_i = 0$. $\|x\|_1$ is the 1-norm of vector $x \in \mathbb{R}^n$, $c_{ij}(t)$ and $c_i(t)$ are adaptive weights, and $\nu \in \mathbb{R}_+$ is a positive control gain. Denoting the estimate error of each agent as $\tilde{v}_i(t) = \hat{v}_i(t) - v_0(t)$, then the error dynamic can be written as

$$\begin{aligned}\dot{\tilde{v}}_i &= - \sum_{j=1}^N c_{ij}(t) a_{ij} \text{sign}(\tilde{v}_i - \tilde{v}_j) \\ &\quad - c_i(t) b_i \text{sign}(\tilde{v}_i) - \dot{v}_0.\end{aligned}\quad (7)$$

As stated in [41], the Filippov solution of (7) is defined as an absolutely continuous solution of the differential inclusion as follows:

$$\dot{\tilde{v}}_i \in \mathcal{K} \left[- \sum_{j=1}^N c_{ij}(t) a_{ij}(t) \text{sign}(\tilde{v}_i - \tilde{v}_j) \right. \quad (8)$$

$$\left. - c_i(t) b_i \text{sign}(\tilde{v}_i) - \dot{v}_0 \right]. \quad (9)$$

Let $\tilde{v} = [\tilde{v}_1^T, \dots, \tilde{v}_N^T]^T$, $c(t) \equiv \text{diag}(c_{ij})$, and $\beta(t) \equiv \text{diag}(c_i)$. We can rewrite (8) as the following matrix-vector form:

$$\begin{aligned}\dot{\tilde{v}} &\in \mathcal{K} \left[-(\mathcal{H} \otimes I_2)(c(t) \otimes I_2) \text{sign}((\mathcal{H} \otimes I_2)\tilde{v}) \right. \\ &\quad \left. - \beta(t) \mathcal{D} \text{sign}(\tilde{v}) - 1_N \otimes \dot{v}_0 \right].\end{aligned}\quad (10)$$

Then, the following convergence result is established.

Theorem 1 (Adaptive Observer): Given the unknown bounded reference $v_0(t)$, the fully distributed adaptive observer in (5) with (6) can asymptotically estimate the reference velocity for each agent under Assumption 1.

Proof: Since the sign function in (5) is discontinuous, non-smooth analysis will be carried out to study its stability. To this end, (5) is written as follows in terms of differential inclusions:

$$\dot{\tilde{v}} \stackrel{a.e.}{\in} \mathcal{K} \left[-(\mathcal{H} \otimes I_2)(c(t) \otimes I_2) \text{sign}((\mathcal{H} \otimes I_2)\tilde{v}) - 1_N \otimes \dot{v}_0 \right] \quad (11)$$

where *a.e.* means “almost everywhere.” Then, consider the following Lyapunov function for (11):

$$\begin{aligned}U_1(t) &= \frac{1}{2} \tilde{v}^T \tilde{v} + \frac{1}{2} \sum_{i=1}^N \sum_{j \in \mathcal{N}_i} \frac{(c_{ij}(t) - c_e^*)^2}{\nu} \\ &\quad + \frac{1}{2} \sum_{i=1}^l \frac{(c_i(t) - c_p^*)^2}{\nu}\end{aligned}\quad (12)$$

where c_e^* and c_p^* are positive constants to be determined later. The set-valued Lie derivative of $U_1(t)$ is given as follows:

$$\begin{aligned}\dot{U}_1(t) &= \tilde{v}^T \mathcal{K} \left[\dot{\tilde{v}} + \sum_{i=1}^N \sum_{j \in \mathcal{N}_i} (c_{ij}(t) - c_e^*) \dot{c}_{ij} \right. \\ &\quad \left. + \sum_{i=1}^l (c_i(t) - c_p^*) \dot{c}_i \right] \\ &= \mathcal{K} \left[-\tilde{v}^T (\mathcal{H} \otimes I_2)(c(t) \otimes I_2) \text{sign}((\mathcal{H} \otimes I_2)\tilde{v}) \right. \\ &\quad \left. - \tilde{v}^T \beta(t) \mathcal{D} \text{sign}(\tilde{v}) - \tilde{v}^T (1_N \otimes \dot{v}_0) \right. \\ &\quad \left. + \sum_{i=1}^N \sum_{j \in \mathcal{N}_i} (c_{ij} - c_e^*) \|\tilde{v}_i - \tilde{v}_j\|_1 \right. \\ &\quad \left. + \sum_{i=1}^l (c_i(t) - c_p^*) \|\tilde{v}_i\|_1 \right].\end{aligned}\quad (13)$$

Note that by using this fact that $\delta \text{sign}(\delta) = \|\delta\|_1$, we have

$$\begin{aligned}\tilde{v}^T (\mathcal{H} \otimes I_2)(c(t) \otimes I_2) \text{sign}((\mathcal{H} \otimes I_2)\tilde{v}) \\ = \sum_{i=1}^N \sum_{j \in \mathcal{N}_i} c_{ij}(t) \|\tilde{v}_i - \tilde{v}_j\|_1\end{aligned}\quad (14)$$

$$\tilde{v}^T \beta(t) \mathcal{D} \text{sign}(\tilde{v}) = \sum_{i=1}^l c_i(t) \|\tilde{v}_i\|_1. \quad (15)$$

In addition

$$\begin{aligned}\tilde{v}^T (1_N \otimes \dot{v}_0) \\ = \tilde{v}^T (\tilde{\mathcal{L}} \otimes I_2)(\tilde{\mathcal{L}}^{-1} \otimes I_2)(1_N \otimes \dot{v}_0) \\ \leq \|(\tilde{\mathcal{L}} \otimes I_2)\tilde{v}\|_1 \|(\tilde{\mathcal{L}}^{-1} \otimes I_2)(1_N \otimes \dot{v}_0)\|_\infty \\ \leq \frac{\gamma}{\lambda_{\min}(\tilde{\mathcal{L}})} \left(\sum_{i=1}^N \sum_{j \in \mathcal{N}_i} \|\tilde{v}_i - \tilde{v}_j\|_1 + \sum_{i=1}^l c_i(t) \|\tilde{v}_i\|_1 \right)\end{aligned}\quad (16)$$

where $\tilde{\mathcal{L}} := \mathcal{L} + \mathcal{D}$ is an invertible matrix, which is ensured by the condition that $\mathcal{G}(\mathcal{V}, \mathcal{E})$ contains a spanning tree from Assumption 1 [43]. Then, combining (13)–(16) yields

$$\begin{aligned}\dot{U}_1(t) &\leq \mathcal{K} \left[- \sum_{i=1}^N \sum_{j \in \mathcal{N}_i} c_{ij}(t) \|\tilde{v}_i - \tilde{v}_j\|_1 - \sum_{i=1}^l c_i(t) \|\tilde{v}_i\|_1 \right. \\ &\quad + \frac{\gamma}{\lambda_{\min}(\tilde{\mathcal{L}})} \left(\sum_{i=1}^N \sum_{j \in \mathcal{N}_i} \|\tilde{v}_i - \tilde{v}_j\|_1 + \sum_{i=1}^l c_i(t) \|\tilde{v}_i\|_1 \right) \\ &\quad + \sum_{i=1}^N \sum_{j \in \mathcal{N}_i} (c_{ij} - c_e^*) \|\tilde{v}_i - \tilde{v}_j\|_1 \\ &\quad \left. + \sum_{i=1}^l (c_i(t) - c_p^*) \|\tilde{v}_i\|_1 \right]\end{aligned}$$

$$\leq \mathcal{K} \left[- \sum_{i=1}^N \sum_{j \in \mathcal{N}_i} \left(c_e^* - \frac{\gamma}{\lambda_{\min}(\bar{\mathcal{L}})} \right) \|\tilde{v}_i - \tilde{v}_j\|_1 - \sum_{i=1}^l \left(c_p^* - \frac{\gamma}{\lambda_{\min}(\bar{\mathcal{L}})} \right) \|\tilde{v}_i\|_1 \right] \triangleq V(t). \quad (17)$$

Choosing $c_e^* > \gamma/\lambda_{\min}(\bar{\mathcal{L}})$, $c_p^* > \gamma/\lambda_{\min}(\bar{\mathcal{L}})$ such that $\dot{U}_1(t) \leq 0$, which directly leads to that $U_1(t)$ is nonincreasing. Then, according to (12) and (17), we have $\tilde{v}(t)$, $c_{ij}(t)$, and $c_i(t)$ are all bounded. Since the reference velocity and its derivative are both bounded, there exists $\gamma \in \mathbb{R}_+$ such that $\|\dot{v}_0\|_\infty \leq \gamma$, which derives that $\tilde{v}(t)$ is also bounded. Therefore, $\lim_{t \rightarrow \infty} U_1(t)$ is also bounded. Recall that (17) ensures that $\int_0^\infty V(\tau) d\tau$ exists and is finite. Under Assumption 2, $\dot{V}(t)$ is thus bounded, which implies that $V(t)$ is uniformly continuous. According to Lemma 2, it yields $\lim_{t \rightarrow \infty} V(t) = 0$ and $\lim_{t \rightarrow \infty} \tilde{v}(t) = 0$. In addition, with $v \in \mathbb{R}_+$, one has $c_{ij}(t)$ and $c_i(t)$ are monotonically increasing and bounded. Thus, $c_{ij}(t)$ and $c_i(t)$ will converge to certain constants. This completes the proof. ■

Remark 2: It is worth noting that the adaptive dynamic control law in (6) only depends on the estimation errors. Thus, there is no need to know the bound of the desired velocity. Unlike the results in [31], [32], and [36], where the control gain design involves the minimal nonzero eigenvalue of \mathcal{L} and the bound of the desired velocity, the velocity estimator in (5) is fully distributed without any global information, including the bound of the desired velocity.

B. Adaptive Bearing-Only Controller Design

In this section, to solve Problem 1, the bearing-only formation tracking control law is designed as follows:

$$\begin{cases} v_i = \|\vartheta_i\| \cos \tilde{\theta}_i \\ \omega_i = -k_i^\theta \tilde{\theta}_i + \dot{\theta}_i^* \end{cases} \quad (18)$$

where $k_i^\theta \in \mathbb{R}_+$ is the control gain, $\tilde{\theta}_i = \theta_i - \theta_i^*$ with

$$\theta_i^* = \begin{cases} \text{atan2}(\vartheta_i^y, \vartheta_i^x), & \text{if } \vartheta_i \neq 0, \\ 0, & \text{if } \vartheta_i = 0 \end{cases} \quad (19)$$

where atan2 is well-known 2-argument arctangent function [44] and $\vartheta_i = [\vartheta_i^x, \vartheta_i^y]^T$ is designed as

$$\vartheta_i = -k_a \sum_{j \in \mathcal{N}_i} P_{g_{ij}}(t) g_{ij}^* + \hat{v}_i \quad (20)$$

with \hat{v}_i being the estimate of the trajectory velocity, which is generated by (5). $k_a \in \mathbb{R}_+$, $P_{g_{ij}}(t)$ is given in (1).

Then, the following result is obtained.

Theorem 2 (Formation Tracking Convergence): Given an infinitesimal bearing rigid target formation $F^*(t) = (\mathcal{G}^*, p(t))$ and desired velocity $v_0(t)$, Problem 1 can be solved using the proposed control laws (18)–(20) under the fully distributed adaptive observer (5) and (6).

Proof: Under the proposed linear velocity control law in (18), the position dynamic can be written as

$$\dot{p}_i = \begin{bmatrix} \|\vartheta_i\| \cos \tilde{\theta}_i \cos \theta_i \\ \|\vartheta_i\| \cos \tilde{\theta}_i \sin \theta_i \end{bmatrix}. \quad (21)$$

According to the definition of ϑ_i , we have

$$\vartheta_i^x = \|\vartheta_i\| \cos \theta_i^*, \quad \vartheta_i^y = \|\vartheta_i\| \sin \theta_i^*. \quad (22)$$

Then, (21) can be rewritten as

$$\begin{aligned} \dot{p}_i &= \begin{bmatrix} \|\vartheta_i\| \cos \tilde{\theta}_i \cos(\tilde{\theta}_i + \theta_i^*) \\ \|\vartheta_i\| \cos \tilde{\theta}_i \sin(\tilde{\theta}_i + \theta_i^*) \end{bmatrix} \\ &= \begin{bmatrix} \|\vartheta_i\| \cos \tilde{\theta}_i (\cos \tilde{\theta}_i \cos \theta_i^* - \sin \tilde{\theta}_i \sin \theta_i^*) \\ \|\vartheta_i\| \cos \tilde{\theta}_i (\sin \tilde{\theta}_i \cos \theta_i^* + \cos \tilde{\theta}_i \sin \theta_i^*) \end{bmatrix} \\ &= Q_{\tilde{\theta}_i} \vartheta_i \end{aligned} \quad (23)$$

where

$$Q_{\tilde{\theta}_i} \triangleq \begin{bmatrix} \cos^2 \tilde{\theta}_i & -\frac{1}{2} \sin 2\tilde{\theta}_i \\ \frac{1}{2} \sin 2\tilde{\theta}_i & \cos^2 \tilde{\theta}_i \end{bmatrix}. \quad (24)$$

Considering system (3), define the formation error as

$$\tilde{g}_{ij}(t) = g_{ij}(t) - g_{ij}^*, \quad (i, j) \in \mathcal{E}. \quad (25)$$

Then, differentiating (25) yields

$$\dot{\tilde{g}}_{ij} = \frac{\partial g_{ij}}{\partial e_{ij}} \frac{\partial e_{ij}}{\partial t} = \frac{P_{g_{ij}}(Q_{\tilde{\theta}_i} v_i - Q_{\tilde{\theta}_j} v_j)}{\|e_{ij}\|}. \quad (26)$$

For agent i , the total local bearing error can be rewritten as follows by removing the distance error $\|e_{ij}\|$ as stated in [24]

$$\dot{\tilde{g}}_i = \sum_{(i,j) \in \mathcal{E}} P_{g_{ij}}(Q_{\tilde{\theta}_i} \vartheta_i - Q_{\tilde{\theta}_j} \vartheta_j). \quad (27)$$

According to the definition of bearing rigid matrix in (2), rewrite (27) into a matrix-vector form as

$$\dot{\tilde{g}} = \mathcal{R}(p) Q_{\tilde{\theta}} \vartheta \quad (28)$$

where $Q_{\tilde{\theta}} = \text{diag}\{Q_{\tilde{\theta}_i}\}$. Since $\vartheta = -k_a \mathcal{B}(p) g^* + \hat{v}$ with $\hat{v} = [\hat{v}_1^T, \hat{v}_2^T, \dots, \hat{v}_N^T]^T$ and $\tilde{v} = \hat{v} - 1_n \otimes v_0$, then

$$\begin{aligned} \dot{\tilde{g}} &= -k_a \mathcal{R}(p) Q_{\tilde{\theta}} \mathcal{R}(p) g^* + \mathcal{R}(p) Q_{\tilde{\theta}} \hat{v} \\ &= -k_a \mathcal{R}(p) Q_{\tilde{\theta}} \mathcal{R}(p) g^* + \mathcal{R}(p) Q_{\tilde{\theta}} (\tilde{v} + 1_n \otimes v_0) \\ &= -k_a \mathcal{R}(p) Q_{\tilde{\theta}} \mathcal{R}(p) \tilde{g} + \mathcal{R}(p) Q_{\tilde{\theta}} (\tilde{v} + 1_n \otimes v_0). \end{aligned} \quad (29)$$

Note that $|Q_{\tilde{\theta}_i}| = \cos^4 \tilde{\theta}_i + 1/4 \sin^2 2\tilde{\theta}_i = \cos^2 \tilde{\theta}_i$.

Next, under the proposed angle velocity control law, we have

$$\dot{\tilde{\theta}}_i = -k_i^\theta \tilde{\theta}_i \quad (30)$$

which yields that $\cos^2 \tilde{\theta}_i \rightarrow 1$ and $Q_{\tilde{\theta}} \rightarrow I_N$.

By examining the closed-loop system (29) and (30), it can be seen as a cascaded system with $x_2 = (\tilde{v}, \tilde{\theta})$ as stated in Lemma 3. Note that $x_2 = (\tilde{v}, \tilde{\theta}) \rightarrow 0$ results in $x_1 = \tilde{g} \rightarrow 0$ by Lemma 3. Meanwhile, according to Lemma 1, the formation shape is uniquely determined by $F^*(t) = (\mathcal{G}^*, p(t))$. Then, we know that $g_{ij} \rightarrow g_{ij}^*$ for all $(i, j) \in \mathcal{E}$ and $v_i(t) \rightarrow v_0(t)$ as $t \rightarrow \infty$. ■

Remark 3: It can be seen that the velocity control law in (20) consists of two parts. The first one is used to maintain the desired formation, while the second one is to maintain the desired velocity. As a special case that $v_0(t) = 0$, when the desired formation achieves, $\vartheta_i = 0$. Since the definition of $\text{atan2}(0, 0)$ does not exist, a switching approach is used to

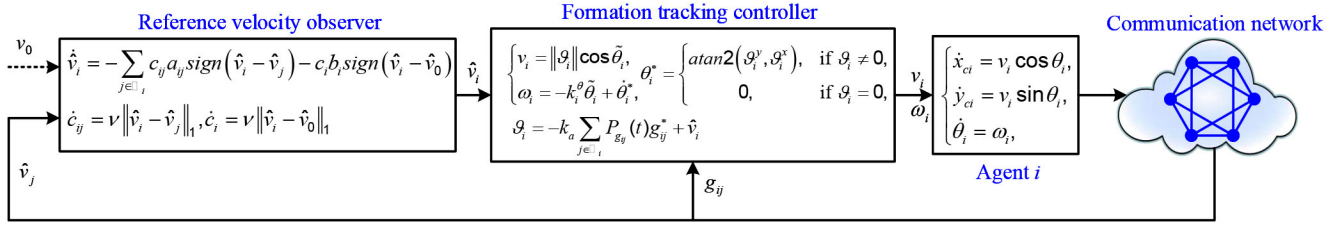


Fig. 2. Illustration of the proposed control scheme.

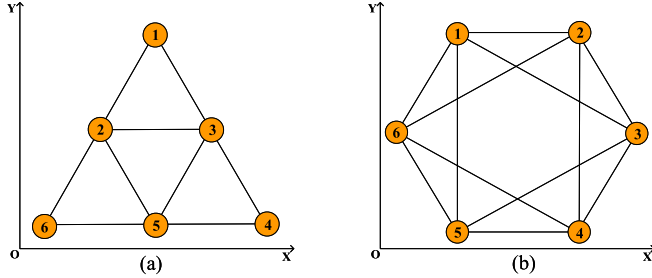


Fig. 3. Two target formations with different configuration containing six agents.

design the desired heading angle control law in (19) so that the point $\text{atan2}(0, 0)$ is excluded. In addition, such a special case will be verified by an experiment in Section IV. To clarify the proposed control scheme, an illustration is given in Fig. 2.

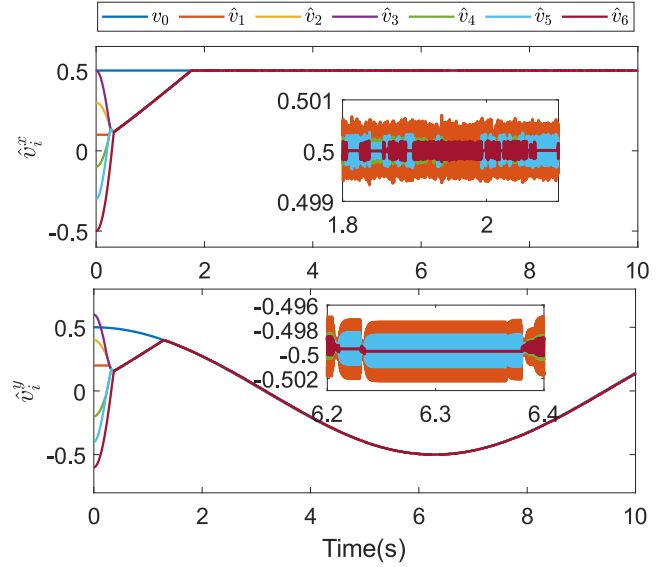
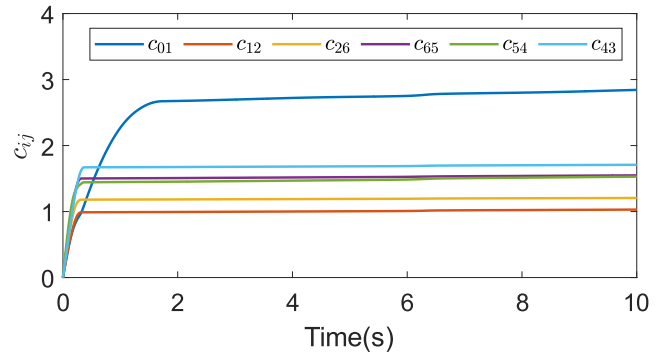
Remark 4: It is worth mentioning that the proposed bearing-only formation tracking control law is globally stable except that $g_{ij}(0) = -g_{ij}^*$, which corresponds to the case that the target formation is rotated 180 degrees. Comparing with [27] and [29], the proposed approach only needs the bearing-only measurements without any limitations on the initial conditions.

IV. SIMULATION AND EXPERIMENT

In this section, some simulations and experimental tests are presented to demonstrate and verify the effectiveness of the proposed adaptive observer and control laws. Since the velocity estimator can be decoupled from the formation tracking control law, we will first verify its effectiveness. Then, the formation tracking control law will be verified by two examples with different configurations. Finally, an experiment will be given to verify the proposed control laws. In these cases, six agents are considered and the target formation is shown in Fig. 3. It can be verified by the rank condition that the target formations in Fig. 3 satisfy Assumption 1. Note that the control parameters in simulation are chosen according to the conditions in Theorems 1 and 2. It can be seen that the proposed results are almost globally stable, which is ensured by selecting positive control gains based on the conditions. Their magnitude will only affect the convergence rate.

A. Fully Distributed Adaptive Observer

We assume that only Agent 1 can access to the desired velocity $v_0(t) = [0.5, 0.5 \sin(0.5t)]$. Under Assumption 1, the communication topology $\mathcal{G}(\mathcal{V}, \mathcal{E})$ obviously contains a spanning tree. For simplicity, only the six edges, that is, $(0, 1)$,

Fig. 4. Velocity estimates \hat{v}_i .Fig. 5. Evolution of $c_{ij}(t)$.

$(1, 2)$, $(2, 6)$, $(6, 5)$, $(5, 4)$, $(4, 3)$, are used. The initial values of the observers are randomly chosen. The initial values of the adaptive parameters c_i are chosen to be 0. The control gain is chosen as $\nu = 5$. Then, by using the adaptive observer in (5) and (6), the results are shown in Figs. 4 and 5. It can be seen that the desired velocity can be estimated by each agent and the adaptive parameters is also convergent as stated in proof of Theorem 1. From Fig. 4, it can be seen that chattering exists in reference velocity estimates, due to the sign function involved in the velocity observer. The chattering will not affect the formation tracking performance, but may lead the control input chattering since the reference velocity estimate is directly used in the control input (20). Note that the chattering caused by the sign function cannot be eliminated,

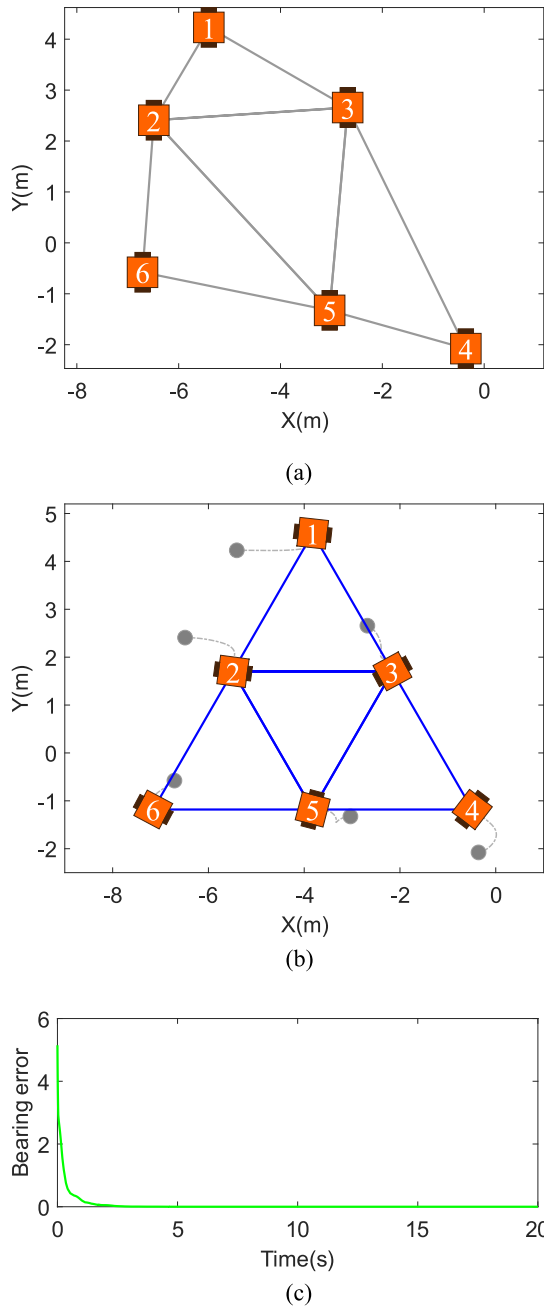


Fig. 6. Formation control for the first configuration in case 1. (a) Initial position of each agent. (b) Formation control and the trajectories of the six agents. (c) Total formation errors.

unless sacrificing the perfect tracking property. A widely used alternative is the use of approximations to the sign function. Saturation and sigmoids functions are often used, offering a continuous or smooth control signal but losing the invariance property of the sliding-mode control. As for how to eliminate the chattering phenomenon is out of the scope of this article and will be considered in the future.

B. Bearing-Only Formation Tracking

In this part, the proposed bearing-only formation tracking control laws will be verified by two cases with the target formations given in Fig. 3.

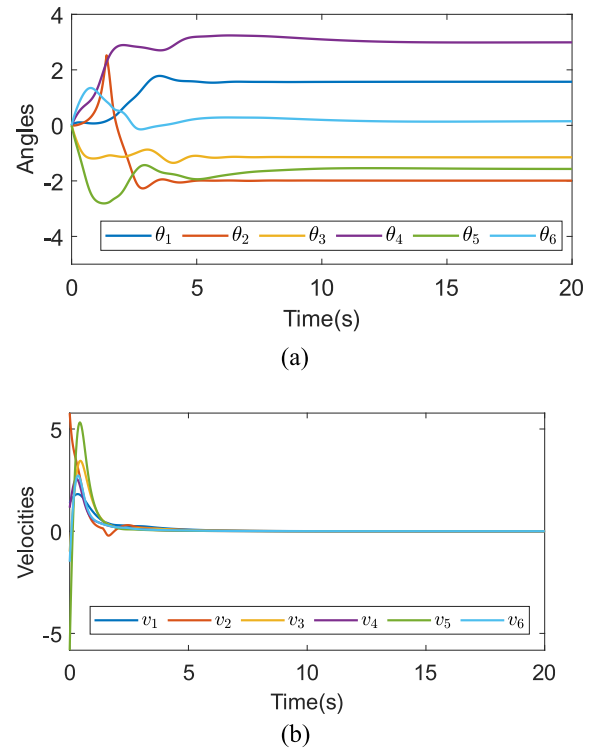


Fig. 7. Heading angles and velocities for the first configuration in case 1. (a) Heading angle of each agent. (b) Velocity of each agent.

Case 1: In this case, the desired velocity is set to be 0, that is, $v_0(t) = 0$. The control parameters are chosen as $k_i^\theta = k_a = 5$. The simulation results are shown in Figs. 6–9. For the first configuration shown in Fig. 3(a), the initial positions and heading angles of the agents are randomly chosen as shown in Fig. 6(a). The initial velocities of the agents are set to be 0. Under the proposed control laws in (18)–(20), the agents converge to the target formation as shown in Fig. 6(b), where the gray lines are the trajectory of each agent. The total formation error given by $\sum_{k=1}^m \|g_k - g_k^*\|$ is shown in Fig. 6(c), which will decay to 0 as the target formation emerging. The heading angles and linear velocities of the agents are given in Fig. 7. It shows that the heading angles converge to some constant and the linear velocities converge to 0 under the proposed control laws.

For the second configuration shown in Fig. 3(b), the simulation results are given in Figs. 8 and 9. The initial positions and heading angles are also randomly chosen, as shown in Fig. 8(a). It can be seen from Fig. 8(b) and (c), under the proposed control laws in (18)–(20), the target formation can be achieved and the total bearing error of the formation reduces to 0. From Fig. 9, the heading angles and velocities of the six agents are also convergent.

Case 2: In this case, the simulation results for dynamic formation tracking are presented. The desired velocity is given by $v_0(t) = [0.5, 0.5 \sin(0.5t)]$, which is estimated by the adaptive observer in (5) and (6) for each agent. The two configurations shown in Fig. 3 are also considered. The control parameters are also chosen as $k_i^\theta = k_a = 5$. For the first target configuration, randomly choosing the initial positions and heading angles of the agents, which can be seen in Fig. 10(a) at $t = 0$ s.

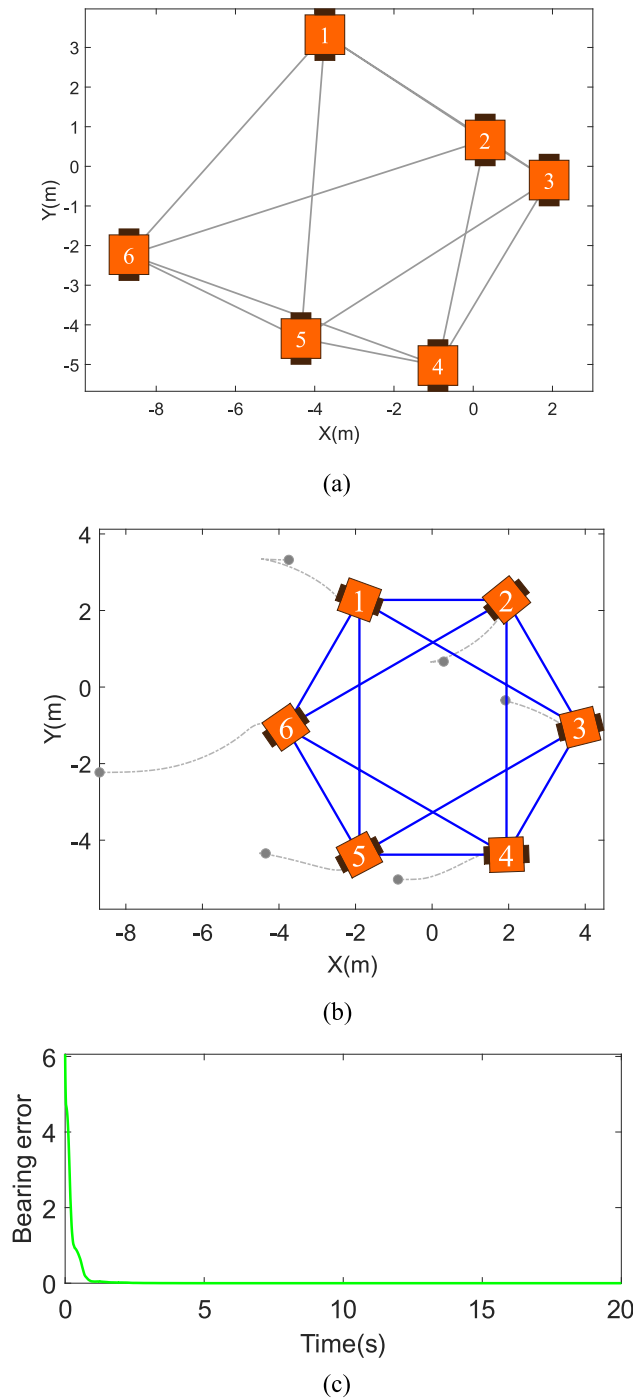


Fig. 8. Formation control for the second configuration in case 1. (a) Initial position of each agent. (b) Formation control and the trajectories of the six agents. (c) Total formation errors.

The formation tracking progress is also shown in Fig. 10(a), where the formation shape at $t = 10$ s and $t = 20$ s are drawn at different moments. Under the proposed control laws in (18)–(20), it can be seen that the nonholonomic multiagent can track the desired velocity by maintaining the target formation shape. The total formation error is given in Fig. 10(b). The heading angles and velocities of the agents are shown in Fig. 11. It can be seen that the heading angles can achieve consensus under the proposed control law. Since the radii of the agents in different positions in the formation are different,

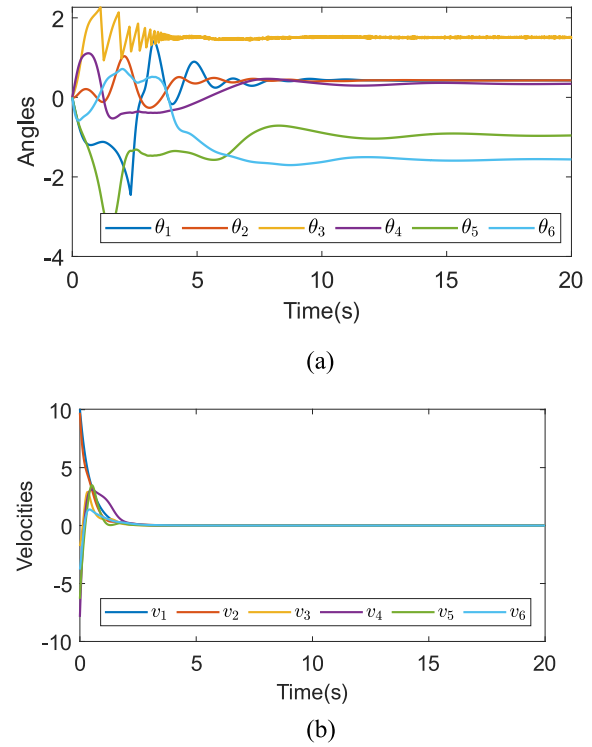


Fig. 9. Heading angles and velocities for the second configuration in case 1. (a) Heading angle of each agent. (b) Velocity of each agent.

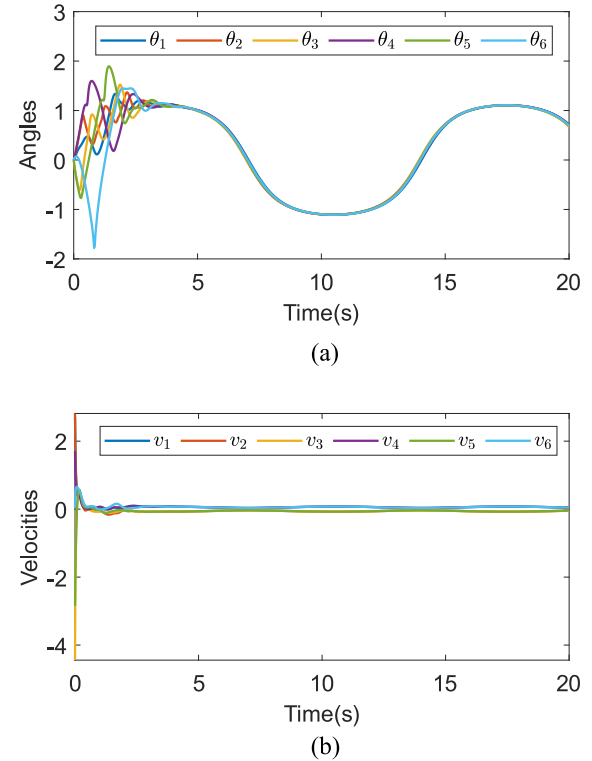


Fig. 10. Formation tracking for the first configuration in case 2. (a) Formation tracking. (b) Total formation error.

the velocities of the agents in Fig. 11(b) produces a grouping phenomenon. These results verify the effectiveness of the proposed control laws.

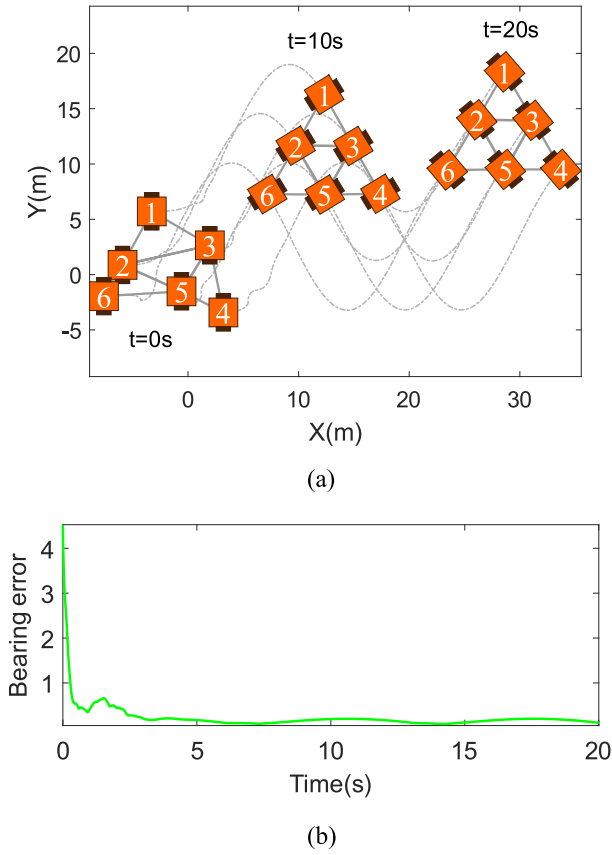


Fig. 11. Heading angles and velocities for the first configuration in case 2. (a) Heading angle of each agent. (b) Velocity of each agent.

For the second configuration shown in Fig. 3(b), with the same control parameters, the formation tracking can also be guaranteed under the proposed control laws in (18)–(20). The simulation results are given in Figs. 12 and 13. From Fig. 12(a), the initial positions, the trajectories, and the final formation shape are given. Correspondingly, the total bearing error is given in Fig. 12(b). The heading angles and velocities are also given in Fig. 13. It can be seen that the formation tracking problem can be solved by the proposed control laws.

C. Experimental Results

In this section, an experimental test is presented by an open-source platform to verify the effectiveness of the proposed control laws. The experiment is performed in Robotarium, which is developed by Georgia Institute of Technology [45], [46]. The system architecture of the multirobot testbeds consists of several parts shown in Fig. 14. It mainly includes local execution components and remote access components. By uploading our algorithm into the Web front end, the control algorithm is verified by the user management and transferred to the server. After downloading our control algorithm to each robot, the six robots are randomly deployed into the workplace. The relative bearings of the robots can be measured by the visual sensor above the experimental platform. In this part, limited by operating space and execution ability, the case that $v_0(t) = 0$ is verified under the proposed control laws.

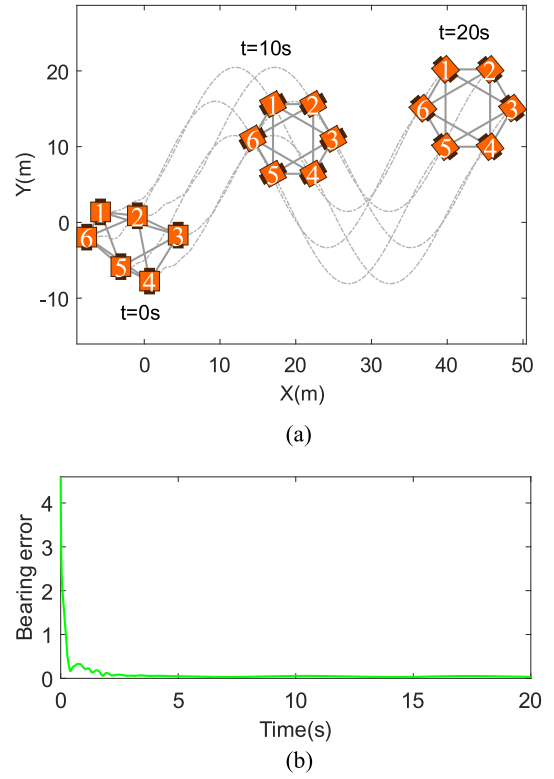


Fig. 12. Formation tracking for the second configuration in case 2. (a) Formation tracking. (b) Total formation error.

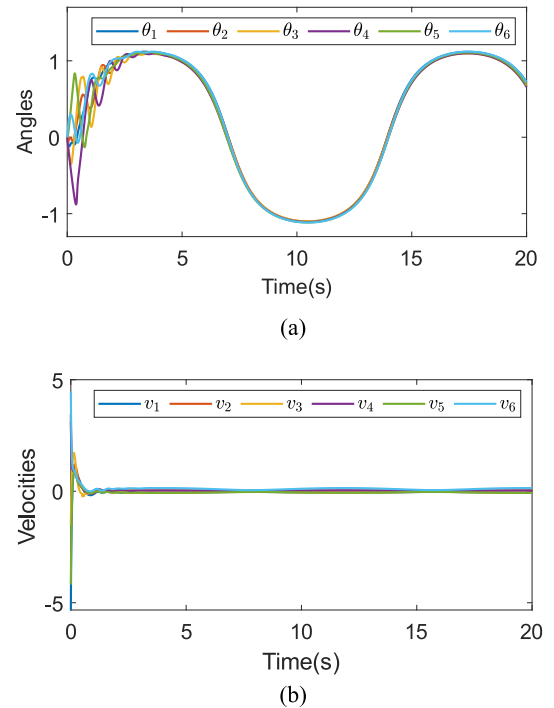


Fig. 13. Heading angles and velocities for the second configuration in case 2. (a) Heading angle of each agent. (b) Velocity of each agent.

The experimental results are shown in Fig. 15. The target formation is similar to the first configuration shown in Fig. 3(a), which is rotated 45° clockwise. The initial positions of the six robots are shown in Fig. 15(a). From Fig. 15(a)–(f), the positions of the six robots at different times

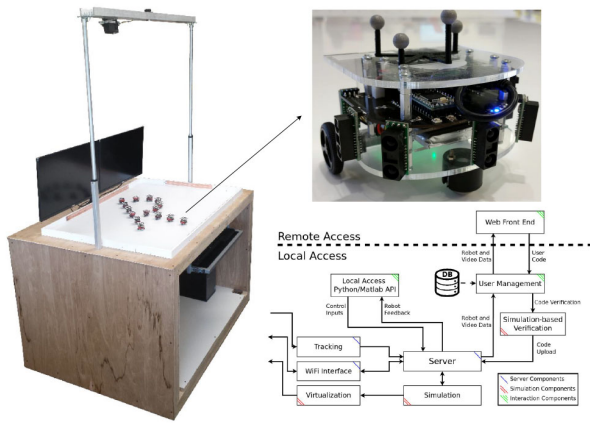
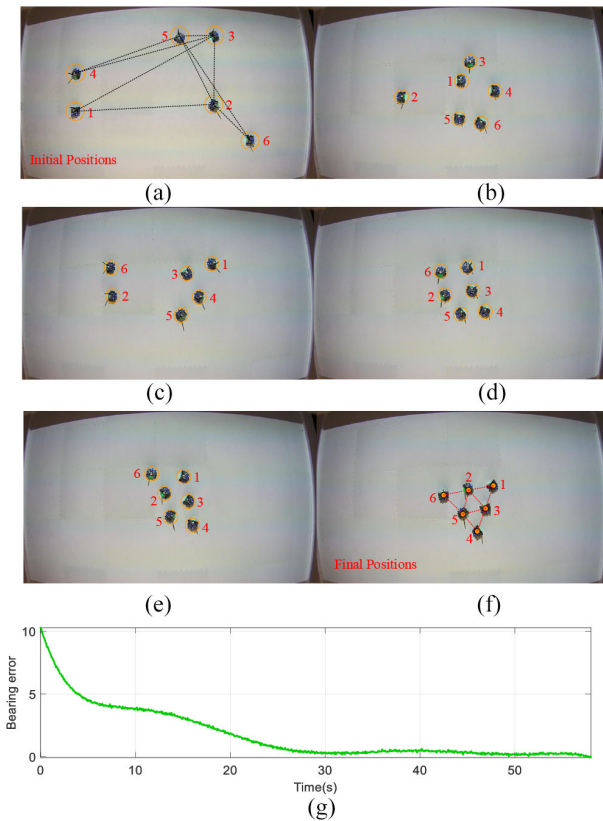


Fig. 14. Opensource multirobot testbeds [45].

Fig. 15. Experimental results with six robots. (a) $T = 0$ s. (b) $T = 12$ s. (c) $T = 31$ s. (d) $T = 40$ s. (e) $T = 50$ s. (f) $T = 58$ s. (g) Formation error.

are given. Under the proposed control laws, the formation can be achieved only using the relative bearing measurements. The total bearing errors of the formation can be seen in Fig. 15(e). Despite the uncertainties, such as measurement noise and system model uncertainty, etc., the formation error is still convergent, which is acceptable in practice. Therefore, the effectiveness of the proposed control law is verified.

V. CONCLUSION

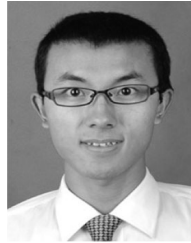
In this article, we considered the bearing-only tracking problem for nonholonomic multiagent systems. A fully distributed adaptive observer was designed such that each agent can estimate the desired velocity without depending on the eigenvalue information of the Laplace matrix and the bound

of the desired velocity. Under the proposed adaptive observer, an input-to-state stable control law was proposed only using the relative bearing measurements of the agents. Then, the bearing-only tracking problem was solved by the proposed observer and controller. Simulation and experimental results were presented to verify their effectiveness. In the future, how to achieve formation tracking for the multiagent systems modeled by a dynamic model is an important and interesting topic. In addition, how to achieve formation control in case that some agents fail is also an interesting topic.

REFERENCES

- [1] A. N. Bishop, M. Deghat, B. D. O. Anderson, and Y. Hong, "Distributed formation control with relaxed motion requirements," *Int. J. Robust Nonlinear Control*, vol. 25, no. 17, pp. 3210–3230, 2014.
- [2] S. Ghapani, J. Mei, W. Ren, and Y. Song, "Fully distributed flocking with a moving leader for Lagrange networks with parametric uncertainties," *Automatica*, vol. 67, pp. 67–76, May 2016.
- [3] F. Boem, Y. Zhou, C. Fischione, and T. Parisini, "Distributed Pareto-optimal state estimation using sensor networks," *Automatica*, vol. 93, pp. 211–223, Jul. 2018.
- [4] P. Xie, K. You, R. Tempo, S. Song, and C. Wu, "Distributed convex optimization with inequality constraints over time-varying unbalanced digraphs," *IEEE Trans. Autom. Control*, vol. 63, no. 12, pp. 4331–4337, Dec. 2018.
- [5] H. Liu, Y. Tian, and F. L. Lewis, "Robust trajectory tracking in satellite time-varying formation flying," *IEEE Trans. Cybern.*, early access, Jan. 9, 2020, doi: [10.1109/TCYB.2019.2960363](https://doi.org/10.1109/TCYB.2019.2960363).
- [6] L. Chen, Z. Sun, C. Li, B. Zhu, and C. Wang, "Satellite affine formation flying with obstacle avoidance," *J. Aerosp. Eng.*, vol. 233, no. 16, pp. 5992–6004, 2019.
- [7] A. González, M. Aranda, G. López-Nicolás, and C. Sagüés, "Robust stability analysis of formation control in local frames under time-varying delays and actuator faults," *J. Franklin Inst.*, vol. 356, no. 2, pp. 1131–1153, 2019.
- [8] D. Wang, Q. Zong, B. Tian, F. Wang, and L. Dou, "Finite-time fully distributed formation reconfiguration control for UAV helicopters," *Int. J. Robust Nonlinear Control*, vol. 28, no. 18, pp. 5943–5961, 2018.
- [9] X. Li, X. Luo, J. Wang, Y. Zhu, and X. Guan, "Bearing-based formation control of networked robotic systems with parametric uncertainties," *Neurocomputing*, vol. 306, no. 6, pp. 234–245, 2018.
- [10] X. Li, C. Wen, and C. Chen, "Adaptive formation control of networked robotic systems with bearing-only measurements," *IEEE Trans. Cybern.*, early access, Mar. 25, 2020, doi: [10.1109/TCYB.2020.2978981](https://doi.org/10.1109/TCYB.2020.2978981).
- [11] K. Xie, C. Chen, F. L. Lewis, and S. Xie, "Adaptive compensation for nonlinear time-varying multiagent systems with actuator failures and unknown control directions," *IEEE Trans. Cybern.*, vol. 49, no. 5, pp. 1780–1790, May 2019.
- [12] C. Song, L. Liu, G. Feng, and S. Xu, "Coverage control for heterogeneous mobile sensor networks on a circle," *Automatica*, vol. 63, pp. 349–358, Jan. 2016.
- [13] L. Dou, C. Song, X. Wang, L. Liu, and G. Feng, "Coverage control for heterogeneous mobile sensor networks subject to measurement errors," *IEEE Trans. Autom. Control*, vol. 63, no. 10, pp. 3479–3486, Oct. 2018.
- [14] Z. Sun, S. Mou, B. Anderson, and M. Cao, "Exponential stability for formation control systems with generalized controllers: A unified approach," *Syst. Control Lett.*, vol. 93, pp. 50–57, Jul. 2016.
- [15] Z. Zhao, Z. Li, and Z. Ding, "Bearing-only formation tracking control of multiagent systems," *IEEE Trans. Autom. Control*, vol. 64, no. 11, pp. 4541–4554, Nov. 2019.
- [16] K. K. Oh, M. C. Park, and H. S. Ahn, "A survey of multi-agent formation control," *Automatica*, vol. 53, no. 3, pp. 424–440, 2015.
- [17] R. Tron, J. Thomas, G. Loianno, and K. Daniilidis, "A distributed optimization framework for localization and formation control: Applications to vision-based measurements," *IEEE Control Syst. Mag.*, vol. 36, no. 4, pp. 22–44, Aug. 2016.
- [18] A. C. Gurbuz, V. Cevher, and J. H. McClellan, "Bearing estimation via spatial sparsity using compressive sensing," *IEEE Trans. Aerosp. Electron. Syst.*, vol. 48, no. 2, pp. 1358–1369, Apr. 2012.
- [19] Y.-M. Chen, J.-H. Lee, C.-C. Yeh, and J. Mar, "Bearing estimation without calibration for randomly perturbed arrays," *IEEE Trans. Signal Process.*, vol. 39, no. 1, pp. 194–197, Jan. 1991.

- [20] A. N. Bishop and M. Basiri, "Bearing-only triangular formation control on the plane and the sphere," in *Proc. 18th Mediterr. Conf. Control Autom. (MED)*, Marrakech, Morocco, 2010, pp. 790–795.
- [21] A. N. Bishop, "Distributed bearing-only quadrilateral formation control," *IFAC Proc. Vol.*, vol. 44, no. 1, pp. 4507–4512, 2011.
- [22] A. N. Bishop, "Distributed bearing-only formation control with four agents and a weak control law," in *Proc. 9th IEEE Int. Conf. Control Autom. (ICCA)*, Santiago, Chile, 2011, pp. 30–35.
- [23] A. N. Bishop, "A very relaxed control law for bearing-only triangular formation control," *IFAC Proc. Vol.*, vol. 44, no. 1, pp. 5991–5998, 2011.
- [24] S. Zhao and D. Zelazo, "Bearing rigidity and almost global bearing-only formation stabilization," *IEEE Trans. Autom. Control*, vol. 61, no. 5, pp. 1255–1268, May 2016.
- [25] D. Zelazo, P. R. Giordano, and A. Franchi, "Bearing-only formation control using an SE(2) rigidity theory," in *Proc. 54th IEEE Conf. Decis. Control (CDC)*, Osaka, Japan, 2015, pp. 6121–6126.
- [26] S. Zhao and D. Zelazo, "Translational and scaling formation maneuver control via a bearing-based approach," *IEEE Trans. Control Netw. Syst.*, vol. 4, no. 3, pp. 429–438, Sep. 2017.
- [27] S. Zhao and D. Zelazo, "Bearing-based formation maneuvering," in *Proc. IEEE Multi-Conf. Syst. Control*, Sydney, NSW, Australia, Sep. 2015, pp. 658–663.
- [28] X. Dong and G. Hu, "Time-varying formation tracking for linear multiagent systems with multiple leaders," *IEEE Trans. Autom. Control*, vol. 62, no. 7, pp. 3658–3664, Jul. 2017.
- [29] H. Liu, Y. Tian, F. L. Lewis, Y. Wan, and K. P. Valavanis, "Robust formation tracking control for multiple quadrotors under aggressive maneuvers," *Automatica*, vol. 105, pp. 179–185, Jul. 2019.
- [30] Q. Yang, M. Cao, H. G. de Marina, H. Fang, and J. Chen, "Distributed formation tracking using local coordinate systems," *Syst. Control Lett.*, vol. 111, pp. 70–78, Jan. 2018.
- [31] M. Khaledyan, T. Liu, V. Fernandez-Kim, and M. de Queiroz, "Flocking and target interception control for formations of nonholonomic kinematic agents," *IEEE Trans. Control Syst. Technol.*, vol. 28, no. 4, pp. 1603–1610, Jul. 2020.
- [32] F. Mehdifar, F. Hashemzadeh, M. Baradarannia, and M. de Queiroz, "Finite-time rigidity-based formation maneuvering of multiagent systems using distributed finite-time velocity estimators," *IEEE Trans. Cybern.*, vol. 49, no. 12, pp. 4473–4484, Dec. 2019.
- [33] S. Zhao and D. Zelazo, "Localizability and distributed protocols for bearing-based network localization in arbitrary dimensions," *Automatica*, vol. 69, pp. 334–341, Jul. 2016.
- [34] X. Li, X. Luo, and S. Zhao, "Globally convergent distributed network localization using locally measured bearings," *IEEE Trans. Control Netw. Syst.*, vol. 7, no. 1, pp. 245–253, Mar. 2020.
- [35] S. Zhao and D. Zelazo, "Bearing rigidity theory and its applications for control and estimation of network systems: Life beyond distance rigidity," *IEEE Control Syst. Mag.*, vol. 39, no. 2, pp. 66–83, Apr. 2019.
- [36] Z. Li, X. Liu, W. Ren, and L. Xie, "Distributed tracking control for linear multiagent systems with a leader of bounded unknown input," *IEEE Trans. Autom. Control*, vol. 58, no. 2, pp. 518–523, Feb. 2013.
- [37] C. Deng and G.-H. Yang, "Distributed adaptive fault-tolerant control approach to cooperative output regulation for linear multi-agent systems," *Automatica*, vol. 103, pp. 62–68, May 2019.
- [38] C. Deng and C. Wen, "Distributed resilient observer-based fault-tolerant control for heterogeneous multiagent systems under actuator faults and DoS attacks," *IEEE Trans. Control Netw. Syst.*, vol. 7, no. 3, pp. 1308–1318, Sep. 2020.
- [39] X.-J. Li and G.-H. Yang, "FLS-based adaptive synchronization control of complex dynamical networks with nonlinear couplings and state-dependent uncertainties," *IEEE Trans. Cybern.*, vol. 46, no. 1, pp. 171–180, Jan. 2016.
- [40] X.-J. Li and G.-H. Yang, "Adaptive fault-tolerant synchronization control of a class of complex dynamical networks with general input distribution matrices and actuator faults," *IEEE Trans. Neural Netw. Learn. Syst.*, vol. 28, no. 3, pp. 559–569, Mar. 2017.
- [41] D. Shevitz and B. Paden, "Lyapunov stability theory of nonsmooth systems," *IEEE Trans. Autom. Control*, vol. 39, no. 9, pp. 1910–1914, Sep. 1994.
- [42] H. K. Khalil, *Nonlinear Systems*, 3rd ed. Upper Saddle River, NJ, USA: Prentice-Hall, 2002.
- [43] C. Godsil and F. Gordon, *Algebraic Graph Theory*, New York, NY, USA: Springer, 2013.
- [44] L. Rade and B. Westergren, *Mathematics Handbook for Science and Engineering*. Berlin, Germany: Springer, 2013.
- [45] S. Wilson *et al.*, "The robotarium: Globally impactful opportunities, challenges, and lessons learned in remote-access, distributed control of multirobot systems," *IEEE Control Syst. Mag.*, vol. 40, no. 1, pp. 26–44, Feb. 2020.
- [46] D. Pickem *et al.*, "The robotarium: A remotely accessible swarm robotics research testbed," in *Proc. IEEE Int. Conf. Robot. Autom. (ICRA)*, Singapore, 2017, pp. 1699–1706.



Xiaolei Li received the B.Eng. and Ph.D. degrees in control engineering from Yanshan University, Qinhuangdao, China, in 2012 and 2018, respectively.

Since 2018, he has been acting as a Research Fellow with the School of Electrical and Electronic Engineering, Nanyang Technological University, Singapore. His current research interests focus on localization and formation control of robotic systems and cyber-security of cyber-physical systems.



Changyun Wen (Fellow, IEEE) received the B.Eng. degree from Xi'an Jiaotong University, Xi'an, China, in 1983, and the Ph.D. degree from the University of Newcastle, Newcastle, NSW, Australia, in 1990.

From 1989 to 1991, he was a Research Associate and then a Postdoctoral Fellow with the University of Adelaide, Adelaide, SA, Australia. Since 1991, he has been with the School of Electrical and Electronic Engineering, Nanyang Technological University, Singapore, where he is currently a Full Professor.

His main research activities are in the areas of control systems and applications, autonomous robotic systems, cyber-physical systems, smart grids, complex systems, and networks.

Prof. Wen was a recipient of a number of awards, including the Prestigious Engineering Achievement Award from the Institution of Engineers, Singapore, in 2005, and the Best Paper Award of IEEE TRANSACTIONS ON INDUSTRIAL ELECTRONICS from the IEEE Industrial Electronics Society in 2017. He is an Associate Editor of *Automatica* and IEEE TRANSACTIONS ON INDUSTRIAL ELECTRONICS, respectively. He is the Executive Editor-in-Chief of *Journal of Control and Decision*. He also served as an Associate Editor of IEEE TRANSACTIONS ON AUTOMATIC CONTROL from 2000 to 2002, and *IEEE Control Systems Magazine* from 2009 to 2019. He has been actively involved in organizing international conferences, playing the roles of the General Chair, the General Co-Chair, the Technical Program Committee Chair, the Program Committee Member, the General Advisor, and the Publicity Chair. He was a Member of IEEE Fellow Committee from 2011 to 2013, and a Distinguished Lecturer of IEEE Control Systems Society from 2010 to 2013.



Xu Fang received the B.Eng. degree in electrical engineering from Beijing Forestry University, Beijing, China, in 2013, and the M.Sc. degree in control theory and control engineering from Beihang University, Beijing, in 2016. He is currently pursuing the Ph.D. degree in electrical and electronic engineering from Nanyang Technological University, Singapore.

His research interests include cooperative control, unmanned systems, network localization, and robot navigation.



Jiange Wang received the master's degree in automation from Yanshan University, Qinhuangdao, China, in 2017, where she is currently pursuing the doctoral degree in control theory and control engineering.

From 2018 to 2020, she was an exchange Ph.D. student with the National University of Singapore, Singapore. Her research interests include cooperative control for multiagent systems and intelligent transportation system.